Martin Weyreuther
Christoph E. Heyde · Michael Westphal
Jan Zierski · Ulrich Weber

MRI Atlas
Orthopedics and Neurosurgery
The Spine

Springer

MRI Atlas
Orthopedics and Neurosurgery
The Spine

Martin Weyreuther
Christoph E. Heyde
Michael Westphal
Jan Zierski
Ulrich Weber

MRI Atlas

Orthopedics and Neurosurgery
The Spine

Foreword by
Prof. Dr. med. Dr. h.c. Karl-Jürgen Wolf

Translated by Bettina Herwig

With 524 Figures in 575 Separate Illustrations

Springer

Authors:
Dr. Martin Weyreuther
Röntgenabteilung, HELIOS Klinik Emil von Behring
Walterhöferstr. 11, 14165 Berlin

Dr. Christoph E. Heyde
Unfallchirurgische Universitätsklinik
Charité Campus Benjamin Franklin
Hindenburgdamm 30, 12200 Berlin

Prof. Dr. Michael Westphal
Bonhoefferufer 13, 10589 Berlin

Prof. Dr. Jan Zierski
Neurochirurgische Klinik
Vivantes Klinikum Neukölln
Rudower Str. 48, 12351 Berlin

Prof. Dr. Ulrich Weber
Orthopädische Universitäts-Klinik,
Charité Campus Benjamin Franklin
Hindenburgdamm 30, 12200 Berlin

Translator:
Bettina Herwig
Hauptstraße 4H
10317 Berlin

Title of the Original German Edition:
MRT-Atlas Orthopädie und Neurochirurgie. Wirbelsäule

ISBN 10 3-540-40285-3

ISBN 10 3-540-33533-1 Springer-Verlag Berlin Heidelberg New York
ISBN 13 978-3-540-33533-7 Springer-Verlag Berlin Heidelberg New York

Library of Congress Control Number: 2006929607

Springer is a part of Springer Science+Business Media
springer.com

Editor: Dr. Ute Heilmann, Heidelberg
Desk Editor: Wilma McHugh, Heidelberg
Cover design: Frido Steinen-Broo, Pau, Spain
Typesetting: Satz-Druck-Service, Leimen
Image Editing: AM-productions GmbH, Wiesloch
Production: LE-TEX Jelonek, Schmidt & Vöckler GbR, Leipzig

Printed on acid-free paper 21/3100/YL 5 4 3 2 1 0

Foreword

Though a fairly recent development in the field of radiology, MRI has successfully established itself in the spectrum of imaging modalities. Insights into the body that, until recently, were inconceivable and that have paved the way for devising new diagnostic and therapeutic options have been made possible by the constant improvement in spatial and anatomic detail resolution and advances in data processing that include improved image reconstruction algorithms. On the other hand, the amount of image information now obtainable with state-of-the-art MR scanners makes it ever more important to provide guidance for radiologists, orthopedic surgeons, traumatologists, and other interested specialists, so that they can find their way through the plethora of details. This is the intention of the atlas presented here: it is a practically oriented guide offering a concise overview of the important aspects of normal spinal anatomy and pathology, MR findings in spinal disease and the postoperative spine as well as therapeutic and surgical approaches. Such a guide is especially important for the spine with its unique and complex anatomic structure and function. The rigorous and uniform organization of the book is the work of a group of dedicated authors from different specialties who offer the reader a systematic overview based on their own vast experience and skills.

An invaluable asset of this book is its concise presentation of important interdisciplinary aspects in dealing with spinal disorders. With its unique format, this atlas guides readers through the fundamentals of spinal anatomy and disease states to better establish diagnostic strategies and surgical management.

In the interest of high-quality patient care, our hope is that many readers will find this atlas a vital source of information in the diagnosis and treatment of their patients.

Professor Dr. med. Dr. h.c. Karl-Jürgen Wolf
Berlin, June 2006

Preface

Magnetic resonance imaging is a computer-assisted diagnostic tool that is well established for numerous indications involving the skeleton and its associated structures. Soon after its clinical introduction in the early 1980's, it became apparent that the application of MRI in the evaluation of normal and abnormal conditions yields widely varying qualitative and quantitative results for different anatomic regions of the locomotor system. The most common indications for MRI in this area are diseases and injuries of the spine and joints, in particular the knee. The significance of MRI for these two skeletal areas is reflected by the fact that knee MRI has largely replaced invasive techniques such as diagnostic arthrography and arthroscopy, while spinal MRI has assumed an important place in therapeutic decision-making, especially in surgical planning.

Inspired by the great interest that the MRI atlas of the knee created in 2003, we decided to compile a similar atlas for the spine. Like its predecessor, the MRI atlas of the spine is the result of interdisciplinary cooperation. Many disorders and injuries of the spine and associated structures are treated by orthopedic surgeons, traumatologists, and neurosurgeons alike, while others are predominantly treated in just one of these specialties. Thus, the decision was made to have orthopedic surgeons/traumatologists, MRI radiologists, and neurosurgeons jointly write this atlas in order to comprehensively discuss all aspects of spinal MRI, particularly its benefits and limitations. As always with such a complex field, the choice of conditions (e.g. tumors or vascular malformations) had to be limited. This may appear arbitrary to some readers, but our selection was necessary to illustrate the role of MRI in exemplary cases and to avoid exceeding the scope of this atlas by including rare diseases.

The presentation of the material should help the reader to quickly identify the most important spinal structures on MR images as a basis for rapidly and efficiently detecting abnormal changes and differentiating them from the normal appearance. Thus, as with the MRI atlas of the knee, the focus is again on the presentation of a carefully selected series of images ranging from the normal appearance to abnormal changes combined with concise information on specific MR sequences and parameters as well as pitfalls. Basic background information on anatomy and pathophysiology is presented here, and the clinical significance of MR findings is discussed in relation to the individual spinal diseases and injuries.

The authors hope that our cooperative approach to spinal MRI successfully reconciles the different aspects of our specialties for a unified approach that enables our readers to make the most effective use of MR findings in treating their patients with spinal disorders.

We thank the staff of our publisher, Springer-Verlag, for their excellent support. Particular gratitude is owed to our secretaries, Miriam Ziegler and

Brigitte Seyd, for their contribution. Finally, our thanks go to Dr. S. Stein, Dr. P. Teller, and in particular Dr. M.C. Dulce, who provided many of the images and helped arrange them systematically.

The Authors
Berlin, June 2006

Table of Contents

1 Normal Anatomy and Variants

1.1 Normal Anatomy

MR Technique

The standard MR protocol for a routine evaluation of the spine always comprises imaging in sagittal and axial planes, while coronal images are necessary only to answer specialized questions.

Typical sequences are T1- and T2-weighted sequences, T2-weighted fast spin echo sequences, which may be supplemented by fat-suppressed sequences.

MR Findings

The signal intensity of the marrow in adult vertebrae varies with its fat content and is high relative to muscle on T1- and T2-weighted images. The presence of residual red marrow decreases the signal on T1 and T2. Cortical bone and ligaments have a very low signal intensity on both T1 and T2. The signal intensity of vessels is low or high, depending on the pulse sequence used and the flow velocity of the blood (cervical spine, Figs. 1.1–1.4; thoracic spine, Figs. 1.5–1.8; lumbar spine, Figs. 1.9–1.12).

1.2 Conjoined Nerve Roots

Anatomy

Conjoined nerve roots are a normal anatomic variant.

MR Technique

Most conjoined nerve roots are discovered incidentally on routine sagittal or axial MR images.

MR Findings

Two adjacent intraspinal nerve roots of normal signal intensity. Both roots emerge at the same level and can be traced to their shared origin. The presence of conjoined nerve roots is characterized by an asymmetrical appearance because no nerve root exits the thecal sac at the level above or below on the same side. Conjoined nerve roots have the same MR signal intensity and contrast enhancement pattern as normal nerve roots (Fig. 1.13).

MR Pitfalls

Conjoined nerve roots may easily be mistaken for disc herniations or free disc fragments.

Clinical Significance

Conjoined nerve roots are normal anatomic variants but are nevertheless important because they are quite common and must not be confused with pathology such as disc sequesters or root neurinoma in patients with clinical symptoms.

1.3 Transitional Vertebra

Anatomy

Transitional vertebrae are vertebrae whose structure features some of the characteristics of the adjacent spinal region. Such indeterminate vertebrae can occur at all spinal junctions and are designated as occipitocervical, cervicothoracic, thoracolumbar, or lumbosacral. There may be complete or incomplete assimilation between adjacent vertebrae.

Pathomechanism

Transitional vertebrae are not considered malformations although they are associated with shifts in the vertical segmentation of the spine. The shift involves not only the bony elements but also muscles, nerves, vessels, and other anatomic structures.

Cranial shift is reported to be more common than caudal shift. The normal numerical distribution of vertebrae (seven cranial, twelve thoracic, five lumbar, five sacral, and four coccygeal vertebrae) is present in only two thirds of individuals. Transitional vertebrae are most common at the lumbosacral junction (lumbarization of the first sacral vertebra, sacralization of the fifth lumbar vertebra).

MR Technique

Transitional vertebrae are best identified on sagittal T1- or T2-weighted images (Fig. 1.14).

Most transitional vertebrae are detected incidentally on MR images. Correct identification of the level of a transitional vertebra is possible only on images showing the entire spine. In most patients, a transitional vertebra is already known from prior radiographs.

Whenever the involved segment cannot be clearly identified, it must be mentioned in the report and a choice must then be made and consistently applied.

Clinical Significance

Transitional vertebrae can be entirely asymptomatic or can impair the overall static stability of the spine or the biomechanical function of individual motion segments and thus predispose to degenerative spinal disorders. This is especially the case when there is only partial assimilation (e.g. incomplete sacralization of the fifth lumbar vertebra). Of particular significance are skeletal abnormalities of the occipitocervical junction. So-called atlas assimilation (partial or complete fusion of the atlas to the occiput) is rare but is associated with considerable dysfunction (osseous torticollis or wryneck) and often causes neurologic deficits (disturbance of the pyramidal tract, Arnold-Chiari malformation).

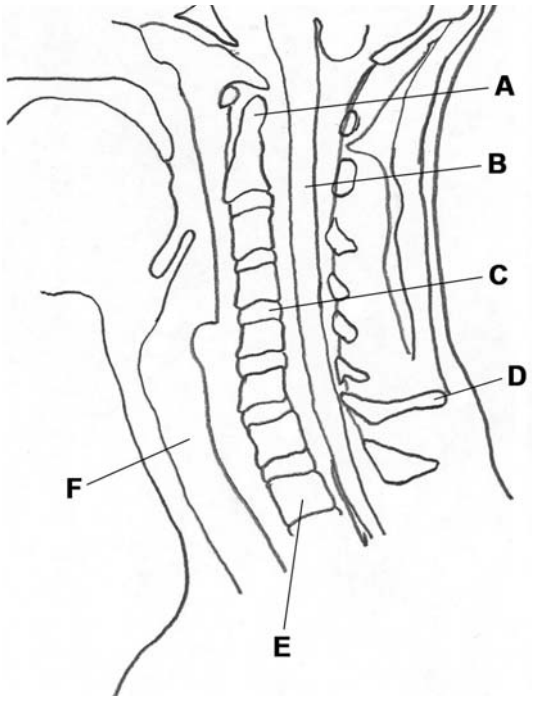

Fig. 1.1. Midline sagittal T1-weighted image of the normal cervical spine obtained with a turbo spin echo (TSE) sequence. Homogeneous appearance of the vertebral marrow. The intervertebral discs are of normal height and nearly isointense to bone. The spinal cord has slightly higher signal intensity relative to the darker cerebrospinal fluid (CSF). A thin layer of soft tissue is depicted anterior to the spine at the level of the epipharynx and pharynx. The soft-tissue-signal structure anterior to the C5 vertebral body represents the proximal portion of the esophagus directly below the glottis. **A** dens axis, **B** spinal cord, **C** C4-5 intervertebral disc, **D** C7 spinous process, **E** T1 vertebral body, **F** trachea

Fig. 1.2. Sagittal T2-weighted TSE image of the normal cervical spine obtained with presaturation of anterior soft tissue structures to eliminate motion artifacts caused by swallowing. The CSF is markedly hyperintense relative to the cord. The vertebral marrow is homogeneous and of similar signal intensity as on T1-weighted images. The CSF appears somewhat inhomogeneous due to pulsation artifacts. The intervertebral discs are of normal height and exhibit some inhomogeneity in signal intensity due to variable fluid content. The posterior neck muscles are clearly seen as low-signal-intensity structures surrounded by fatty tissue

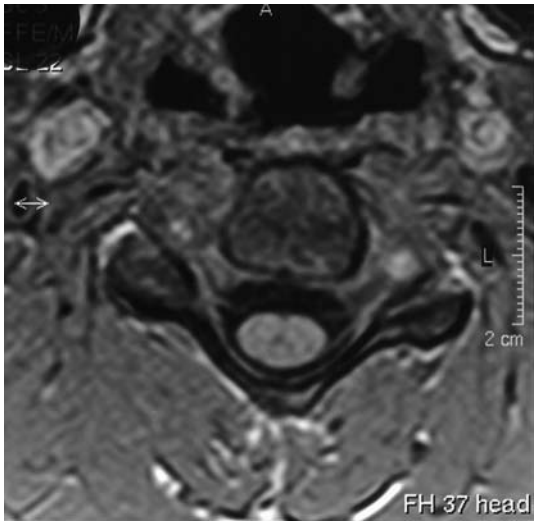

Fig. 1.3. Axial T1-weighted TSE image of the cervical spine through the C4-5 level. There is good visualization of both C5 neural foramina. The spinal nerve roots exiting anteriorly at an angle of about 45° are not very well appreciated on sagittal images. Within the foramina the nerve roots and spinal nerves are seen as low-signal-intensity structures in the bright fatty tissue. The spinal cord has an oval configuration and is well defined by its high signal intensity relative to the surrounding CSF. The posterior portions of the vertebral arch are depicted as delicate bony structures outlined by a dark rim of cortical bone. The vessels are ill-defined relative to surrounding soft tissue

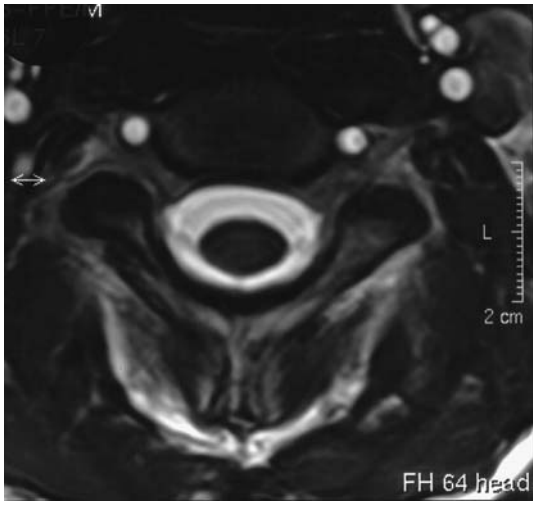

Fig. 1.4. Axial T2-weighted image of the cervical spine through the C3-4 level obtained with a gradient echo (GRE) sequence. There is good differentiation of the bright CSF and dark, homogeneous spinal cord. Note the bright vessel signal, which is typical of GRE sequences

Fig. 1.5. Sagittal T1-weighted image of the thoracic region. Reliable identification of the individual thoracic vertebrae is possible only on images that also visualize portions of the cervical or lumbar spine. The long spinous process at the top is that of C7 (prominent vertebra), thus the spinal region shown extends from C7-T1 to the mid-L2 level. The signal intensities of the different structures are the same as in the cervical region. The epidural fatty tissue posterior to the dural sac is visualized more clearly. The black structure extending down to the T6 level in front of the spine is the air-filled trachea

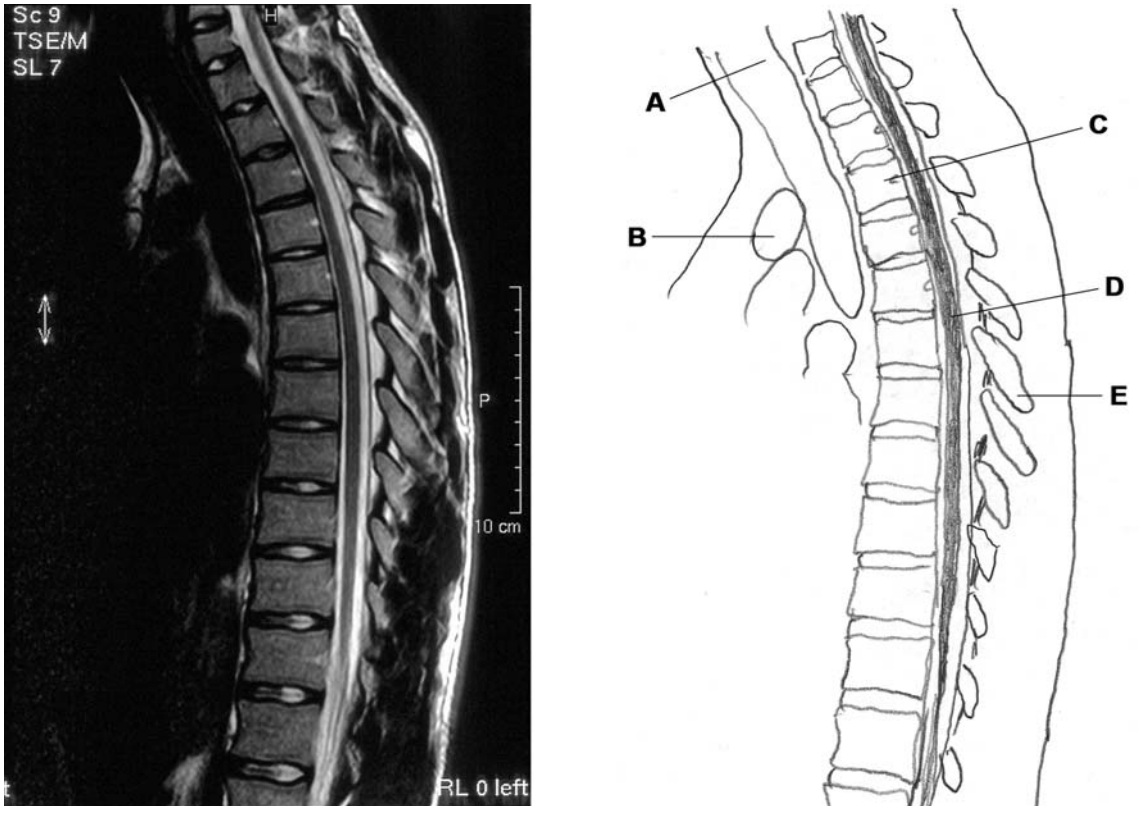

Fig. 1.6. Sagittal T2-weighted image of the thoracic region from C7-T1 to mid-L2. Normal signal intensities of the vertebrae, spinal cord, and soft tissue. Fat and CSF are of the same signal intensity and are separated only by a thin dark line, the dura. **A** trachea, **B** supra-aortic vessels, **C** T3 vertebra, **D** spinal cord, **E** spinous process

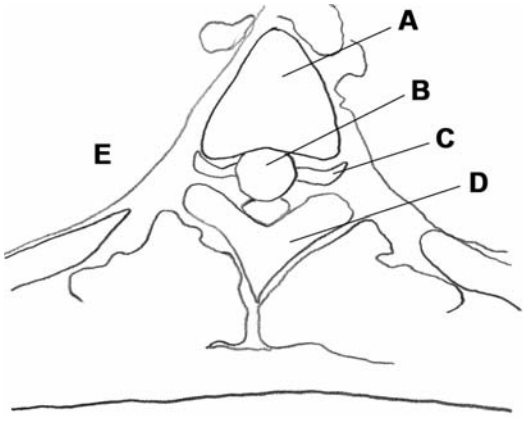

Fig. 1.7. Axial T1-weighted image of the thoracic spine at the level of the T8-9 neural foramina. In relation to the transverse diameter, the anteroposterior diameter of the thoracic vertebral bodies is greater than that of the cervical vertebrae. The nerve roots emerge at an angle of approximately 90°. Within the foramina, the nerve roots are identified by their low signal relative to the bright fatty tissue. The extensor and other back muscles are seen as low-signal-intensity structures relative to fatty tissue in the individual muscle compartments and fasciae. The black areas to the right and left of the vertebral body are the air-filled lungs, which emit no signal. **A** T8 vertebral body, **B** dural sac, **C** left T8 nerve root, **D** vertebral arch/spinous process, **E** lung

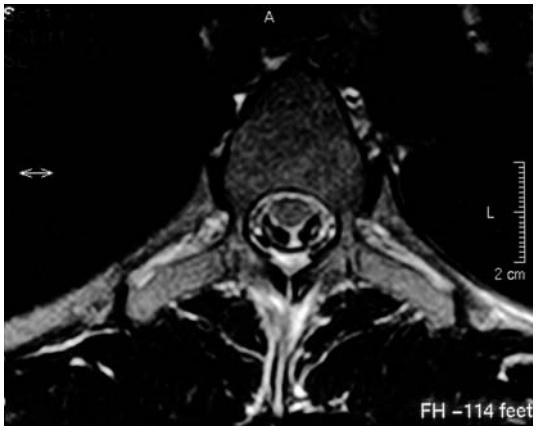

Fig. 1.8. Axial T2-weighted image of the thoracic spine through the T9 level. The pedicles above the neural foramina and the transverse processes are depicted with normal bone signal. The costotransverse joints and portions of the ribs are clearly visible next to the vertebral body and transverse processes. The elongated areas of reduced signal intensity seen in the CSF posterolateral to the cord represent pulsation artifacts

Fig. 1.9. Midline sagittal T1-weighted image of the lumbar spine from T9-10 through S2. The conus medullaris is identified as a slight enlargement of the cord at the T11-12 level. The more delicate nerve fibers of the cauda equina are seen below the conus. Normal appearance and signal intensities of the intervertebral discs and bone

Fig. 1.10. Axial T2-weighted image through the L4-5 level. The neural foramina are oriented anteriorly at an angle of approximately 80°. The facet processes extend posteriorly at an angle of about 45%. The width of the foramina at this level is delimited posteriorly by the facet joints and anteromedially by the disc/L5 endplate. The structures seen posterior to the facet joints are the posterior elements including the spinous process of the L4 vertebra

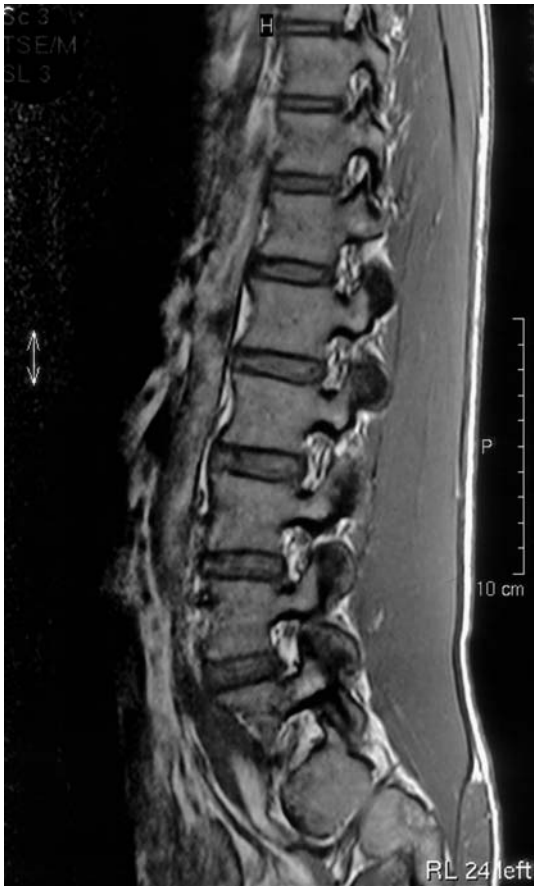

Fig. 1.11. Left parasagittal T1-weighted image of the lumbar spine at the level of the neural foramina. The foramina have an oval configuration with a greater superoinferior diameter. They mostly contain fat in which the spinal nerve roots are discernible as low-signal-intensity punctate structures, typically located in the upper third. The abdominal aorta is seen anterior to the lumbar spine, roughly from T12 through L3-4, as an inhomogeneous vascular structure of mostly high signal intensity. Posterior to the spine, the strong back extensor muscles are depicted as a wide band of intermediate signal intensity beneath the subcutaneous fatty tissue layer

Fig. 1.12. Axial T2-weighted image of the lumbar spine at the L4 level. The Y-shaped hyperintensity in the L4 vertebral body represents venous channels that drain into the epidural veins. The cauda equina fibers are visualized as punctate structures of low signal intensity within the bright CSF. The strong psoas muscle is seen to the right and left of the vertebral body. The inferior vena cava is depicted anterior and to the right of the vertebra adjacent to the two proximal common iliac arteries

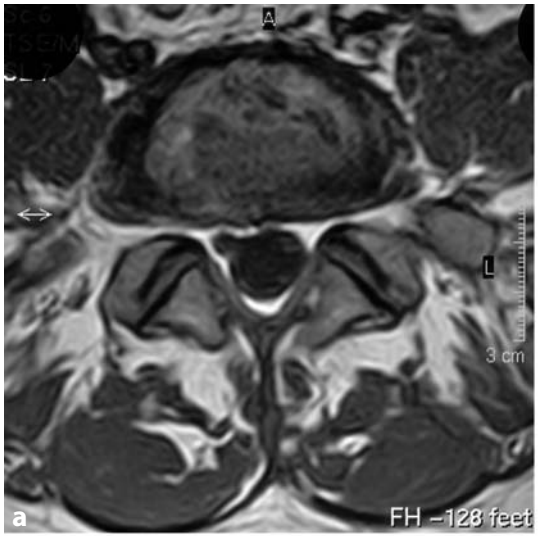

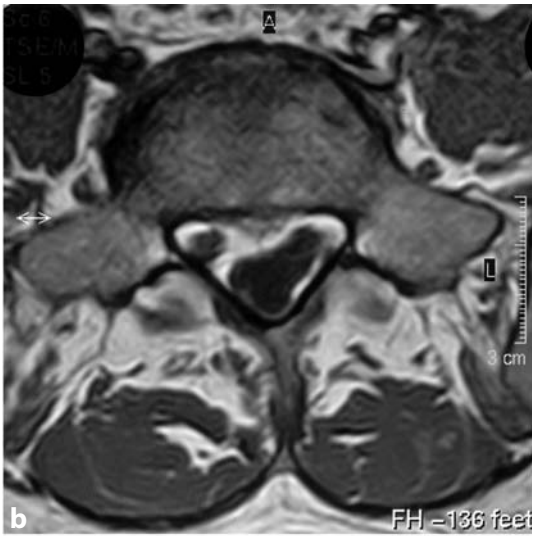

Fig. 1.13a–c. Axial T1-weighted images at the L4-5 and L5 levels. The images illustrate the asymmetrical appearance of the thecal sac resulting from the presence of conjoined L5 and S1 nerve roots on the left

a At this level, only the right L5 nerve root is seen while there is no corresponding root on the left

b The L5 and S1 nerve roots on the left emerge at the same level and are seen as an oval mass

c Both nerve roots are depicted intraspinally to the left of the thecal sac as masses of low signal intensity. On the right, only the L5 nerve root is visualized while the S1 root about to emerge is seen only as an outpouching of the thecal sac

Fig. 1.14. Sagittal T2-weighted image of the lumbar spine and thoracolumbar junction. There is lumbarization of S1 and the lowest intervertebral disc is therefore that of the S1-2 segment. In addition, there are marked degenerative changes of the lower lumbar spine with posterior intervertebral disc herniations at the L3-4 and L4-5 levels

2 Congenital and Developmental Anomalies

2.1 Spinal Meningeal Cysts

The following types are distinguished according to Nabors

Type I	spinal extradural meningeal cysts without spinal nerve root fibers
Type Ia	extradural meningeal cysts
Type Ib	occult intrasacral meningoceles
Type II	spinal extradural meningeal cysts with spinal nerve root fibers
Type III	spinal intradural meningeal cysts (meningeal diverticula)

Pathoanatomy and Pathophysiology

Congenital arachnoid cysts develop from diverticula of the arachnoid mater and communicate with the subarachnoid space. However, a direct communication may not be seen on MRI in all cases. Arachnoid cysts increase in size by a valve mechanism.

Intradural arachnoid cysts most commonly occur in the thoracic spine but may also be found in the lumbar or cervical region. They are lined with arachnoidal cells (type III cysts).

Extradural arachnoid cysts without nerve root elements: type I cysts.

A disorder of secondary neurulation may give rise to a so-called terminal ventricle, a saclike expansion of the central canal of the spinal cord within the conus medullaris.

Extradural meningeal cysts with nerve root fibers (type II, Tarlov cysts) arise from the dorsal ganglion between the arachnoid membrane of the dorsal nerve root (perineurium) and the outer layer of the pia (endoneurium). These cysts are typically multiple and communicate with the subarachnoid space. They often expand the intervertebral foramina and cause smooth erosion of the posterior surface of the vertebral body.

MR Technique

Spinal meningeal cysts can be detected on MR images in all three planes (sagittal, coronal, and axial) and are typically found incidentally (Figs. 2.1–2.14).

MR Findings

Spinal meningeal cysts are depicted on T2-weighted images as sharply demarcated lesions with fluid signal along the course of the spinal nerve roots. The cysts do not enhance after contrast administration. Long-standing cysts may expand the surrounding bony structures (neural foramina).

Clinical Significance

Extradural cysts present with signs of spinal cord compression.

There is controversy about the clinical relevance of Tarlov cysts. Such cysts are often detected incidentally and it is often difficult to establish an association between a patient's clinical symptoms and the cyst. Symptoms are due to other changes in most cases and only very few patients require surgical management.

MR Pitfalls

Meningeal cysts must be differentiated from synovial cysts of the facet joints, which may have the same signal intensity but typically attach to the adjacent articular cavity.

2.2 Bony Malformations

Pathomechanism

Malformations of the bony spine or a spinal segment may be formally classified as:

- segmentation anomalies,
- fusion anomalies,
- defects (formation anomalies), and
- mixed forms (undifferentiated).

The spinal column is derived from the middle layer of the three primary germ layers of the embryo (mesoderm), more specifically from the paraxial mesoderm.

The axial mesoderm develops to form the notochord, thereby defining the longitudinal axis of the body.

So-called somites are paired, blocklike masses that form in the paraxial mesoderm and are arranged segmentally alongside the neural tube, thereby giving rise to a metameric arrangement. Functionally, each somite consists of a so-called dermomyotome (developing into skeletal muscles and connective tissue) and a sclerotome (developing into vertebrae and ribs). Thus, each mesodermal somite gives rise to a spinal motion segment comprising an intervertebral disc and two facet joints (except for the junctional regions) and the adjacent bony structures. The future vertebrae (vertebral body, pedicles, and laminae) form by resegmentation of the somites, which separate into two halves. These original halves then unite with adjacent half segments in such a way that the lower half of one old segment joins with the upper half of the old segment below, forming the primitive vertebra. In this way, the future spinal segments are shifted by half a segment relative to their original metameric arrangement. The development of a normal bony spine relies on both undisturbed horizontal fusion of the paired protovertebral segments (in the regions of the vertebral bodies and arches) and undisturbed vertical fusion.

2.3 Hemivertebra, Wedge Vertebra, Butterfly Vertebra, and Hemimetameric Segmental Shift

Pathoanatomy

Congenital anomalies of the vertebrae may range from mild wedge deformity to complete absence.

Complete absence of a vertebral body is extremely rare, while variable degrees of incomplete development are rather common. There is controversy about the existence of anterior hemivertebrae.

A rudimentary vertebral body may show partial or complete fusion with one or both of its neighbors and the intervening disc may be hypoplastic.

Hemimetameric segmental shift, or segmental displacement, is defined as the presence of two contralateral hemivertebrae which may be separated by one or more normal vertebrae.

As with other vertebral defects, the different forms of rudimentary vertebrae that have just been outlined are often associated with other congenital anomalies (diastema, tethered cord, condylar hyperplasia, basilar impression, and others).

Sagittal cleft vertebral bodies are attributed to the presence of separate ossification centers in the two paired chondrification centers. Similar clefts have also been found in the anterior arch of the atlas.

Sagittal clefts may be complete or incomplete. An incomplete vertebral cleft may affect either the anterior or the posterior portion of the vertebral body. More commonly, there are two notches, one in the superior and one in the inferior endplate, giving rise to the typical butterfly appearance on radiographs.

Pathomechanism

Vertebral anomalies such as hemivertebrae are classified as formation defects while hemimetameric segmental shift, based on current understanding, is attributable to deranged resegmentation of the sclerotomes into vertebrae during early embryonic development.

Butterfly vertebrae result from horizontal fusion defects.

MR Technique

Hemivertebrae and wedge vertebrae are best appreciated on coronal and sagittal images but secondary scoliosis/kyphosis, which is present in the majority of cases, may preclude full evaluation of the spine on a single sagittal image. MRI is performed with T1- and T2-weighted sequences with T2-weighted images often providing a better overview of anatomy in children.

MR Findings

Hemivertebrae/wedge vertebrae have the normal bone marrow signal that varies with the ratio of fat to red marrow. The different vertebral anomalies – hemivertebra, wedge vertebra, and butterfly vertebra – can be distinguished on the basis of their characteristic shapes. Oblique axial images angled parallel to the intervertebral disc space are usually helpful in obtaining true axial images of the vertebral body (Figs. 2.15–2.17).

MR Pitfalls

In most cases, the patient's history will help differentiate congenital vertebral anomalies from posttraumatic vertebral defects. Adequate evaluation of the shape and size of abnormal vertebrae and their arrangement requires careful selection of sagittal and axial slices and images obtained in oblique axial orientation.

Clinical Significance

Abnormal vertebrae may contain large amounts of cartilage due to delayed ossification. In such cases, MRI can diagnose true vertebral deformities even before the completion of growth.

Associated anomalies must be excluded before surgery (basilar impression, diastematomyelia), especially in patients with formation defects of the vertebrae.

Lateral hemivertebrae may lead to congenital mechanical scoliosis, which differs from other forms of scoliosis in that torsion is minimal. Kyphosis may develop when only the posterior portion of a vertebra is present. The smaller the size of the residual vertebral body, the more severe the expected kyphotic or scoliotic deformity. This is why very early surgical correction (in infancy) may be required when the residual vertebral body is reduced to half or less of its normal size. This holds true especially for posterior hemivertebrae since short kyphotic curves (unlike scoliotic deformities) virtually always compromise the spinal canal and bear the risk of later damage to neural structures. In such cases, a wedge vertebra acts as an anterior hypomochlion.

Differentiation of a sagittal cleft vertebra from a sagittal burst fracture is usually straightforward on radiographs and no additional modalities such as MRI are necessary.

The examiner should also look for associated malformations (e.g. abdominal or urogenital).

An isolated sagittal cleft vertebra does not require treatment.

2.4 Klippel-Feil Syndrome

This condition was first described by Klippel and Feil in 1912 and is characterized by shortness of the neck resulting from complete or incomplete fusion of multiple or all cervical vertebrae. The number of cervical vertebrae may also be reduced. The syndrome is typically associated with other anomalies such as Sprengel's deformity, cervical ribs and other rib anomalies, lipoma and angioma in the posterior neck, cervical spina bifida, congenital scoliosis and kyphosis, and basilar impression.

Pathomechanism

Developmental disorder (malsegmentation) inherited as an autosomal dominant trait.

MR Technique

The cervical anomalies associated with Klippel-Feil syndrome are best seen on sagittal and coronal T1- and T2-weighted images. Axial images are less important. Additional sagittal and coronal T2-weighted images with fat saturation are useful to evaluate adjacent discs for signs of osteochondrosis and degenerative changes of the inferior and superior endplates. Fat-suppressed images are more sensitive in demonstrating bone marrow edema typically present in Klippel-Feil syndrome.

MR Findings

MRI shows the extent of fusion of the cervical vertebrae and other changes such as degeneration of preserved disc spaces and disc herniation, which are more common in patients with Klippel-Feil syndrome. Moreover, patients with synostosis of two or more cervical segments also have a higher incidence of other deformities (platybasia, syringomyelia, encephalocele, facial and cranial asymmetry, and Sprengel's deformity in about 25-40% of cases).

Coronal and axial images may fail to show fusion of the posterior elements, which is best appreciated on sagittal images.

MR Pitfalls

Posttraumatic syringomyelia with bony changes may resemble the cervical deformities seen in Klippel-Feil syndrome.

Clinical Significance

In most patients, conventional radiographs are sufficient to diagnose Klippel-Feil syndrome. MRI has a role in identifying the underlying cause in infants presenting with torticollis.

There are no effective therapeutic approaches to correct the unnatural position of the head and limited range of motion. Nevertheless, therapeutic measures may occasionally be indicated if the deformities cause neurologic deficits (cervical spinal canal stenosis, syringomyelia, basilar impression).

2.5 Atlantoaxial Instability and Basilar Impression

MR Technique

Sagittal and axial T1- and T2-weighted images.

MR Findings

Atlantoaxial Instability
Atlantoaxial instability is characterized by increased mobility at the junction between the atlas and the axis. It is defined as an atlantoaxial distance greater than 3 mm in adults and greater than 4 mm in children. Spinal compression myelopathy may occur when the distance is 10 mm or greater.

The atlantoaxial distance can be measured on axial and sagittal images, while concomitant rupture of the annular ligament can only be detected on axial images. Rheumatoid arthritis is characterized by inflammatory tissue in the widened joint space, which shows enhancement on postcontrast images. Erosion of the dens is identified by an altered signal and shape on sagittal T1- and T2-weighted images. Myelomalacia is indicated by areas of increased signal within the spinal cord on T2-weighted images.

The MR appearance of atlantoaxial instability is illustrated in Figs. 2.18 to 2.20. In the example shown, there is marked narrowing of the spinal canal at the C2 level due to anterior displacement of the skull.

Basilar Impression
Projection of the dens tip more than 5 mm above a line connecting the dorsal edge of the hard palate and the posterior border of the foramen magnum (Chamberlain's line) constitutes basilar impression (Figs. 2.21 and 2.22).

MR Pitfalls

Platybasia is also associated with occipitalization of the dens axis (Fig. 2.23) but is a distinct entity. By definition, platybasia exists if the angle between the anterior base of skull and the clivus is greater than 140 degrees (normal range, 125 to 140 degrees).

2.6 Os Odontoideum

Pathoanatomy and Pathophysiology

Os odontoideum is an anomalous bone above a hypoplastic dens that is not attached to the atlas and may occasionally show incomplete fusion with the clivus. It is considered a congenital anomaly, but some authors attribute this condition to a missed dens fracture in infancy.

Os odontoideum may be asymptomatic or present with symptoms in patients with concomitant atlantoaxial instability. This constellation is more common in conjunction with trisomy 21, Klippel-Feil syndrome, or calcifying chondrodystrophy. Instability is due to laxity of the cruciate ligament. Soft tissue forming around an os odontoideum has a similar morphologic appearance on MR images as pannus tissue and may impinge on the spinal cord.

MR Technique

Sagittal and coronal T1- and T2-weighted images and T2 STIR images.

MR Findings

MRI demonstrates an oval or round ossicle with a smooth border. Both the ossicle and dens are imaged with normal bone marrow signal surrounded by a cortical layer of low signal intensity (Fig. 2.24).

MR Pitfalls

Os odontoideum must be differentiated from acute fractures of the dens, which are characterized by the presence of sharp-edged, matching fragments with an altered signal of the fracture margins. In contrast, os odontoideum is typically oval in configuration with smooth borders, and there are no associated soft tissue or spinal cord injuries.

Clinical Significance

Symptoms may first occur after trauma. Patients with incidentally detected os odontoideum and without signs of instability or clinical symptoms should undergo regular clinical follow-up. Posterior instability is treated with C1-2 fusion.

While MRI is not the method of choice for diagnosing os odontoideum, it is indispensable for identifying cervical cord impingement in patients without clinical signs of myelopathy.

2.7 Block Vertebra with Disc Atresia

Pathoanatomy

Congenital block vertebrae are characterized by the partial or complete fusion of two or more adjacent vertebrae due to failure of vertebral segmentation. The intervening disc is rudimentary or absent. When there is incomplete fusion, the affected vertebral bodies are usually normal in shape and height. In complete fusion, deficient growth leads to reduced height, narrow sagittal diameter, and concave anterior configuration. If the corresponding vertebral arches, articular processes, and spinous processes are not fused or if fusion is confined to anterior vertebral portions, affected patients have short kyphotic curves. The rudimentary discs often show calcification on radiographs. In contrast, unilateral failure of segmentation (unilateral unsegmented bar) causes congenital scoliosis.

Pathomechanism

Fusion of one or more vertebrae is attributed to the reduced expression of the Pac-1 gene, a segmentation gene of the family of developmental control genes which is assumed to ascertain the integrity of the discs and spinal segments during spinal development.

MR Technique

Sagittal and coronal T1- and T2-weighted images (Figs. 2.25–2.27).

Clinical Significance

MRI provides important diagnostic information to differentiate congenital vertebral fusion with rudimentary or absent discs from acquired conditions. Normal appearance of the surrounding soft tissue structures, intact endplates, a reduced sagittal diameter of the vertebral bodies, and a concave anterior vertebral surface suggest a congenital defect. Isolated block vertebrae that do not alter the shape of the vertebral column have no clinical relevance. However, as with loss of mobility in individual spinal segments due to other causes, the changes associated with congenital vertebral fusion can also lead to the development of secondary arthrosis resulting from altered stresses at adjacent levels. Surgical treatment may be required for biomechanical reasons if block vertebra is associated with kyphotic deformity or – in rare cases – if there is clinically significant secondary stenosis of the spinal canal due to a short kyphotic curve.

Congenital scoliosis due to unilateral fusion (unilateral bar) tends to have an unfavorable prognosis and may require early surgical management.

2.8 Split Cord Malformations (Diastematomyelia)

Pathoanatomy and Pathophysiology

Diastematomyelia is a congenital anomaly in which the spinal cord is split into halves. Each hemicord has a pair of ventral and dorsal nerve roots and is contained in its own dural sac. The term diplomyelia refers to the complete duplication of the spinal cord with four pairs of nerve roots in a single dural sac. In contrast to earlier assumptions, these two malformations appear to have a similar embryogenesis, which is why the term split cord malforma-

tion should be used for both forms with type I denoting diastematomyelia with a bony spur and type II denoting diplomyelia with a thin fibrous septum. A duplicated or split cord develops if there is dorsal migration and herniation of the endomesenchymal tract into the area of the neural tube. This is why type I split cord malformation may be associated with cleft vertebra (bifid vertebra) or neurenteric cysts of endodermal origin. Whether type I or type II malformation develops, depends on whether the cells of the neural tube split into medial or lateral cell clusters. All split cord malformations have a mesenchymal midline component, either a fibrous strand or vessels coursing along the midline. If the endomesenchymal tract migrates all the way to the skin ectoderm, a dermal sinus will develop with a tract extending from the body surface to the bony spur and hypertrichosis in this area. As a result of migration of the endomesenchymal tract, a broad connection persists between the dura and ectoderm, which explains the coexistence of split cord malformation and open myelomeningocele. In addition, many patients with split cord malformation have associated vertebral anomalies with scoliosis.

MR Technique

Axial T1- and T2-weighted images, which may be supplemented by sagittal and coronal images. GRE sequences are more suitable for demonstrating a bony spicule or septum separating the split or doubled cord. In addition, a CT scan of the affected region may be required.

MR Findings

MR images show the typical appearance of a split spinal cord with tethering and hydromyelia (Figs. 2.28–2.33).

MR Pitfalls

Hydromyelia and syringomyelia may be mistaken for diastematomyelia, especially on sagittal and coronal MR images. This is important to bear in mind particularly because there is an association between diastematomyelia and these two entities.

CT is more reliable in evaluating a bony or connective tissue spur or septum. In many cases, however, it is not possible to differentiate type I and II split cord malformations because images will not show whether one or two separate dural sheaths are present.

Clinical Significance

Skin stigmata on the back should always alert the physician to the possibility of split cord malformation. The clinical symptoms are caused by adhesions and tethering of the cord. Even patients with only mild but progressive symptoms should be operated on before irreversible damage occurs.

2.9 Syringohydromyelia

Pathoanatomy and Pathophysiology

Syringomyelia denotes a pathologic condition characterized by longitudinally oriented CSF cavities within the spinal cord. The term is restricted to this condition and should not be used to designate similar entities such as cysts with a high protein content (e.g. tumor cysts), a terminal ventricle, or residues of the central canal occasionally seen on MR images. The term hydromyelia refers to the cystic dilatation of the ependyma-lined central canal by CSF. However, the syrinx may dissect into the parenchyma of the spinal cord and its original connection with the central canal may disappear. Moreover, the type of lining is also not a reliable criterion to distinguish syringomyelia and hydromyelia. Because of these difficulties, the term syringohydromyelia has been introduced as a convenient term to refer to both entities.

A distinction is made between communicating and noncommunicating syringomyelia, depending on whether the syrinx cavity has a connection to the fourth ventricle. Only 10% of the lesions are of the communicating type. Communicating syringomyelia is often associated with hydrocephalus or complex malformations of the posterior cranial fossa such as Chiari II or Dandy-Walker cysts.

The exact pathomechanism underlying the occurrence of syringomyelia is not clear and various theories have been advanced. Two popular explanations are the hydrodynamic theory, proposing that syringomyelia results from a “water hammer”-like transmission of pulsatile CSF pressure, and a theory that assumes a differential between intracranial and spinal pressure caused by a valvelike action at the foramen magnum. The second of these theories does not adequately account for the occurrence of noncommunicating syrinx cavities.

A further mechanism has been proposed to explain syringomyelia associated with malformations at the

craniocervical junction. Here it is assumed that CSF is forced into the spinal canal through perivascular spaces as a result of pulsation-related pressure differences in the subarachnoid space. This is also the preferred mechanism to explain syringomyelia developing in the presence of posttraumatic adhesions. In the past, posttraumatic syringomyelia used to be interpreted as residual intramedullary hematoma. Moreover, this mechanism can also account for the development of syrinx cavities after infarction or intramedullary bleeding.

Syringomyelia is present in about 65% of patients with Arnold-Chiari I malformation, and it is assumed that narrowing of the subarachnoid space at the craniocervical junction is responsible for this association. The factors contributing to partial or complete obstruction of the subarachnoid space around the medulla oblongata with subsequent development of a syrinx in patients with Chiari I malformation are platybasia, basilar invagination, and a small bony posterior cranial fossa. Syringobulbia is the extension of syrinx cavities into the medulla oblongata.

MR Technique

Sagittal and axial T1- and T2-weighted images. Contrast-enhanced T1-weighted images should be acquired to exclude a tumor.

MR Findings

Demonstration of a syrinx cavity in the spinal cord – whether in the cervical or the lumbar region – should prompt an MRI examination of the entire CNS. In patients scheduled for surgery, it is recommended to assess CSF flow on an electrocardiography-triggered pulse sequence.

MR images rarely enable differentiation of hydromyelia (dilatation of the central canal by CSF) and syringomyelia (intramedullary fluid collection adjacent to the central canal). Both entities are characterized on MRI by the presence of a longitudinally oriented fluid collection in the spinal cord. The lesion is depicted with CSF signal on axial, sagittal, and coronal images.

Congenital or posttraumatic syringohydromyelia does not show contrast enhancement. Tumor-associated syrinx cavities occur inferior to the tumor. Thus, an intramedullary tumor is suggested if an enhancing lesion is seen at the upper end of a fluid collection on T1-weighted images (Figs. 2.34–2.44).

Clinical Significance

Syringomyelia is characterized by slow clinical progression and the syrinx cavities may exist for years without becoming symptomatic. The aim of surgical management is to correct the assumed underlying mechanism. Decompression of the posterior cranial fossa with enlargement of the cisterna magna is the method of first choice. Attempted correction of the associated deformity with decompression is also the primary operative approach in patients with posttraumatic syringomyelia and adhesions, tethered cord, or spinal deformity. Shunting of the syrinx to the subarachnoid space should only be performed in cases where these surgical measures fail or are not an option. The size and extent of a syrinx cavity do not always correlate with a patient's clinical symptoms.

2.10 Spinal Dysraphism

Classification

A distinction is made between open and occult spinal dysraphism. Myelomeningocele is the most common major form of open spinal dysraphism. The second category encompasses meningocele, dermal sinus, lipoma, thickened filum terminale, split cord malformations, and neurenteric cysts.

Clinically, this heterogeneous group of neural tube defects is characterized by tethering of the cord. A subgroup comprises the different forms of lumbosacral agenesis (e.g. terminal myelocystocele) associated with complex urogenital and intestinal anomalies.

Pathoanatomy and Pathomechanism

Dysraphic malformations result from deranged neurulation. The neural tube fails to close and persists as a neural plate (so-called placode). As a result, the superficial ectoderm cannot separate from the neural ectoderm and remains in the lateral position. The skin therefore also develops laterally, leaving a midline defect. Moreover, the mesenchyma is prevented from migrating around the neural tube, resulting in concomitant midline defects of the vertebral arches,

muscles, and ligaments. The placode is surrounded from both sides by an outpouching of the anterior arachnoid membrane. Motor and sensory nerve roots emerge from the ventral surface of the placode. The dura mater is preserved ventrally while its dorsal portion blends into the skin at the edge of the defect. Hence, the meninges and placode are contiguous with the skin. An indentation in the dorsal surface of the placode corresponds to the open central canal at the site of the defect. The central canal above the defect is often widened, and extensive hydromyelia may be present in severe cases.

Over 90% of patients with myelomeningocele have associated deformities of the brain stem, cerebellum, and the upper cervical spinal cord. This complex of deformities is known as Chiari type II malformation and may range from slight rostral displacement of the spinal cord with the upper cervical nerve roots coursing cranially to severe forms with inferior displacement and kinking of the medulla oblongata behind the upper cervical cord, downward displacement of portions of the fourth ventricle and cerebellum into the spinal canal, and deformity of the mesencephalic tectum. By the age of 10, scoliosis is present in about 80% of patients with myelomeningocele, in half of them with a Cobb angle of over 20°. Scoliosis is due to associated vertebral body defects and neuromuscular disorders. Other concurrent conditions include increased lumbar lordosis, thoracic kyphosis, and lumbar kyphosis.

MR Technique

Imaging using T2- and T1-weighted pulse sequences is performed in three planes to determine the site and extent of the deformity. More specifically, MRI serves to evaluate the size and content of the neurocele and to exclude concomitant defects. In patients scheduled for surgery, MR findings provide the basis for planning the surgical approach. In the postoperative follow-up, MRI is performed to exclude retethering and iatrogenic cord ischemia.

MR Findings

MR images show dysraphic lesions of the spinal cord, bony spine, and soft tissues as well as intracranial deformities (Figs. 2.45–2.47).

MR Pitfalls

Confirmation or exclusion of postoperative retethering of the cord may be impaired by the fact that it is often difficult to distinguish strands of scar tissue and nerve roots.

Clinical Significance

Spinal MRI is not required in the primary management of patients with myelomeningocele and merely serves to document the local findings. Patients who show posttherapeutic deterioration of neurologic deficits should undergo repeat MRI to confirm or exclude retethering as a cause of progressive scoliosis. Other lesions that must be excluded are progressive epidermoid tumors, hydromyelia, and arachnoid cysts.

2.11 Tethered Cord

Pathoanatomy and Pathophysiology

Tethered cord is a condition in which the spinal cord is attached to an immobile structure such as the dura, skin, lipoma, or bony vertebral canal.

Between 8 and 25 weeks of gestation, the conus medullaris "ascends" because the bony vertebral column grows faster longitudinally than the spinal cord. As a result of these differences in growth velocity, the conus medullaris terminates at the L2-3 intervertebral disc level at birth and reaches its final height at L1-2 at the age of one.

Pathophysiologically, lesions or dysfunction more commonly affect the spinal cord than the caudal nerve roots. Clinical symptoms are often precipitated by growth spurs in children and activities involving sudden stretching of the spinal column in adults.

MR Technique

Sagittal and axial T1- and T2-weighted images.

MR Findings

MR imaging shows thinning and stretching of the conus medullaris and termination below the L2 level.

Also demonstrated is a conspicuously tense filum terminale, often with thickened fibers (Figs. 2.48–2.51).

Clinical Significance

Tethering of the spinal cord is associated with a very heterogeneous group of congenital anomalies. It presents with characteristic clinical symptoms such as sensory deficits, paresis and muscle atrophy of the legs, pain, urinary and rectal dysfunction, and spinal deformities such as kyphoscoliosis. However, the symptoms differ in children and adults. Concurrent lesions in patients with primary tethered cord are dermal sinus, split cord malformation (diastematomyelia), intraspinal tumors, meningocele and meningomyelocele, intraspinal lipoma, dermoids, and epidermoids.

Patients with cord tethering associated with occult spinal dysraphism have a thick and short filum terminale, often with fat infiltration. A filum terminale lipoma is assumed only if the diameter of the filum terminale is increased to over 2 mm. The mere presence of fatty tissue without tethering or clinical symptoms is a normal variant.

The most common causes of secondary tethering are postinfectious adhesions, trauma, and intradural surgery. Secondary tethering differs from primary tethered cord in that the cord is attached at a different level and not by the filum terminale.

2.12 Scoliosis

Anatomy and Pathoanatomy

Scoliosis is the lateral curvature of the spinal column and is typically associated with spinal torsion due to rotation of vertebrae. Among the few forms of scoliosis without a rotational element is scoliosis secondary to lateral hemivertebrae.

The lateral curve and especially the associated torsion lead to typical changes of the paravertebral structures. In the thoracic region, for example, vertebral rotation also includes the ribs, giving rise to a posterior rib hump on the convex side and an anterior hump on the concave side. Other pathoanatomic changes are specific to the etiology of the different types of scoliosis.

Pathomechanism

The pathogenesis of scoliotic deformities is extremely heterogeneous. A basic distinction can be made between structural and nonstructural forms (functional scoliosis, postural anomalies, improper posture). Structural, or fixed, curves are due to vertebral deformities (wedge vertebra). Typical examples of nonstructural, or mobile, scolioses are reactive forms due to pain (e.g. from disc herniation) and compensatory scoliosis (pelvic tilt).

The pathogenesis of structural scoliosis varies with the age of onset (juvenile versus adult onset). Structural scoliosis in children and young adults is typically due to abnormal growth of the bony spine secondary to vertebral defects (see overview below). In contrast, the underlying pathologic process itself causes the deformity in most forms of adult scoliosis (vertebral destruction due to trauma, inflammation, degenerative lumbar scoliosis). About 95% of the structural scolioses occurring in children and juveniles are of the idiopathic type (right convexity of the thoracic spine).

Forms of Scoliosis

- Neuropathic scoliosis, e.g. meningomyelocele
- Myopathic scoliosis, e.g. muscular dystrophy
- Osteopathic scoliosis, e.g. scoliosis due to formation defects
- Scoliosis due to connective tissue disorders, e.g. Marfan's syndrome
- Other symptomatic scolioses
  - e.g. posttraumatic, postinfectious, and actinogenic scolioses
- Idiopathic scolioses

MR Technique

Coronal and sagittal T1- and T2-weighted images. Full evaluation of the spine in patients with scoliotic curves usually requires sequential imaging of individual regions that are similar in orientation.

MR Findings

Bridging osteophytes on the concave side of the curvature are better appreciated on CT scans. On MR images, osteophytic structures are depicted as thin cortical bands of low signal intensity. In most forms of scolio-

sis, MRI will show mild to severe asymmetries of the vertebral bodies (hemivertebrae). Osteochondrosis of the endplates predominantly involves the concave side. Osteochondrotic changes are isointense with fluid in the acute stage (Modic type 1) and isointense with fat in the chronic stage (Modic type 2). The chronic sclerotic stage (Modic type 3) is characterized by low signal intensity in all sequences. The abnormal stresses associated with scoliotic curves often cause asymmetric enlargement of the facet joints and may lead to stenosis of the spinal canal.

Scoliosis is also associated with a higher risk of disc herniation (Figs. 2.52–2.56).

Clinical Significance

Radiography is the primary diagnostic modality in evaluating patients with scoliosis. MRI is a supplementary tool and mainly serves to demonstrate or exclude concomitant changes in neural structures or the spinal canal (diastema, basilar impression, spina bifida) including the neural foramina. Therefore, MRI is mainly performed in cases where such changes are likely to be encountered (e.g. congenital scoliosis) and when the scoliotic deformity causes clinical symptoms such as pain (reactive scoliosis secondary to vertebral osteoid osteoma). In patients scheduled for surgery, MRI (or CT) findings are helpful in planning the surgical procedure because they enable exact evaluation of vertebral body rotation and assessment of the shape and size of the pedicles. The latter information is important to assess whether the pedicles are suitable as anchorage sites for transpedicular osteosynthesis. However, MRI has no role in the vast majority of patients with clinically and radiographically diagnosed scoliosis.

2.13 Kyphosis

Pathoanatomy

Kyphosis is defined as an abnormally increased posterior convexity of the vertebral column as viewed from the side. Kyphotic deformities of the spine also include loss of normal cervical and lumbar lordosis (hypolordosis).

Multiple wedge deformities of adjacent vertebral bodies and/or intervertebral discs give rise to a smooth kyphotic curve, which must be distinguished from kyphosis with a sharply angled curve (gibbus deformity). Wedge-shaped deformities are shared by all forms of kyphosis, while additional anatomic abnormalities vary with the underlying cause.

Pathogenesis

Apart from congenital defects, any longer-lasting or permanent instability resulting from the loss of anterior support or posterior tension band function (see overview below) will inevitably cause a kyphotic deformity. In the upright posture, the spine is constantly being pulled forward by the weight of the body, exposing all motion segments to a bending force, which can be converted to axial load only by the posterior tension band in conjunction with intact anterior support.

Causes of Kyphosis
- Congenital anomalies (failure of segmentation)
- Formation defects
- Scheuermann's disease
- Paralysis
- Meningomyelocele
- Traumatic damage
- Inflammatory destruction
- Defects secondary to surgery (laminectomy, spondylectomy) or radiotherapy
- Metabolic bone disease (storage diseases, mucolipidosis, Hurler's syndrome)
- Osteochondrodysplasia
- Collagen diseases
- Tumors
- Neurofibromatosis

Clinical Significance

Spinal stenosis due to narrowing of the bony canal or anterior displacement of the spinal cord is much more common in patients with kyphotic deformities than in patients with scoliosis. MRI is currently the most suitable imaging modality for evaluating the anterior, epidural, and subarachnoid reserve space both in the initial diagnostic work-up and follow-up of patients with kyphotic curves. In addition, MRI provides information on intramedullary abnormalities (myelomalacia, syringomyelia).

2.14 Lipomatosis and Lipoma

Pathoanatomy and Pathophysiology

Spinal lipomas are attributed to a developmental disorder caused by the premature focal disjunction of the epidermal and neural ectoderm before closure of the neural tube. As a result, mesenchymal tissue becomes contiguous with the posterior neural tube, which is assumed to induce subsequent differentiation of the mesenchymal tissue into fatty tissue.

Subdural lipomas found beneath an intact dura are also ensheathed by pia mater. The bulk of the mass is usually located posterior to the spinal cord and impinges on it.

Lipoma of the Filum Terminale

The most common form of lipoma of the filum terminale is a lipomyelomeningocele with the fatty mass arising from the dorsal aspect of the cord and extending below the skin. Terminal lipoma is associated with a defect in the dura mater. The subcutaneous fatty mass is apparent at birth. The lesion is covered by intact skin but skin stigmata are often present. The topographic relationship to the nerve roots is variable – the latter may course directly through the lipoma. There is a nearly 100% association of lipomyelomeningocele with tethered cord and termination of the conus medullaris at an abnormal level.

MR Technique

Multiplanar imaging including fat-suppressed sequences encompassing the lumbar, sacral, and coccygeal regions.

MR Findings

MRI shows the extent of spinal lipoma and concomitant defects.

Clinical Significance

MRI is the method of choice to fully evaluate changes in subcutaneous fatty tissue and the topographic relationship of a lipoma to the vertebral canal and spinal cord.

Surgical removal may also be indicated for prophylactic reasons. Complete removal of a lipoma from the conus medullaris region is almost impossible. The major challenge is to prevent retethering of the cord. Based on morphologic MR criteria, it may be very difficult or even impossible to identify postoperative retethering because there will be adherence of neural structures to the dura in virtually all cases. This is why the diagnosis of retethering primarily relies on a patient's clinical course.

2.15 Scheuermann's Disease

Pathoanatomy

Scheuermann's disease, or adolescent kyphosis, is characterized by wedging of one or more adjacent vertebral bodies, scalloping of vertebral endplates, disturbed anterior vertebral growth, and herniation of intervertebral disc tissue into an adjoining vertebra (Schmorl's node). These changes can occur together or alone and involve the middle and lower thoracic spine and the upper lumbar region. Because the vertebral defects (wedging and scalloping) develop during the growth phase, there may be compensatory molding of adjacent vertebrae.

Pathogenesis

The vertebral changes seen in Scheuermann's disease are due to osteochondrosis of the secondary ossification centers of the vertebral bodies (endplate and annular epiphyses). It is still debated whether Schmorl's nodes represent residues of the cartilaginous endplates resulting from circumscribed developmental defects or whether they actually consist of disc tissue extending through gaps in the cartilaginous endplates. A genetic basis is assumed (dominant trait with low penetrance).

MR Technique

The typical lesions occurring in Scheuermann's disease are evaluated on coronal and sagittal T1- and T2-weighted images. Acute changes of vertebral endplates with concomitant edema of the surrounding bone marrow are best seen on fat-saturated T2-weighted images.

The lesions are less prominent on axial images, which must be angled parallel to the endplates of affected vertebral bodies in patients with kyphotic or scoliotic deformities.

MR Findings

Full-blown spinal osteochondrosis, or juvenile kyphosis, is characterized on MRI by the presence of vertebral defects comprising wedging, contour irregularities of the endplates, and narrowing of the disc spaces. The defects most commonly involve the lower thoracic and upper lumbar regions. The slightly increased anteroposterior diameter of the vertebral bodies is best appreciated on sagittal images, which will also demonstrate the loss of the normal lordotic curvature and the severity of kyphotic deformity. Schmorl's nodes are depicted as gaps with marginal sclerosis in the endplates. The herniated disc material typically has a slightly lower signal intensity on T2-weighted images but the signal intensity may also be slightly higher, depending on the age of the herniation. Bone marrow edema around the herniated tissue suggests an acute process (Figs. 2.57–2.61).

MR Pitfalls

Developmental defects of the anterior vertebral bodies may have a similar appearance as in Scheuermann's disease, while wedge deformities and Schmorl's nodes are absent. Bone dystrophies also involve the extremities, which are unaffected in Scheuermann's disease.

Clinical Significance

In rare cases may it be difficult to distinguish Scheuermann's disease from other entities. For example, large destructive tumors, in particular chondrogenic tumors, may resemble large isolated areas of disturbed ossification in Scheuermann's disease.

In such cases, MRI shows concomitant changes of the adjacent vertebral endplates, pronounced reactive marginal sclerosis around the defect, and signs of reactive growth of adjacent vertebrae.

Disc space narrowing with a concomitant defect in an adjacent inferior endplate is also present in spondylodiscitis. In patients with these MRI findings, Scheuermann's disease is suggested if laboratory testing shows normal inflammatory parameters and only mild clinical symptoms are present. The most important distinguishing feature, however, is the visualization of circumscribed, dense zones of sclerosis around the endplate defects on MR images. Sclerosis is absent in florid inflammation and shows diffuse extension into the vertebral body in the presence of a chronic inflammatory process.

It is open whether conservative therapeutic measures aimed at relieving the spine (e.g. specific exercises or a reclination corset) during florid disease will slow down the progression of vertebral wedging and kyphotic deformity.

MRI performed after the acute stage can identify additional typical lesions, thereby contributing to the differentiation of Scheuermann's disease from posttraumatic wedge vertebrae. Most importantly, the microstructure of the cancellous vertebral bone is preserved in Scheuermann's disease.

2.16 Hemangioma

Pathoanatomy

Hemangiomas are capillary or cavernous tumors that are characterized by proliferation of endothelial cells. Vertebral hemangiomas have a characteristic appearance on conventional radiographs (CT scans) resulting from the presence of vertically oriented trabecular bone structures. MRI (and pathohistologic examinations) has shown that the typical radiographic appearance can be caused by two distinct lesions: intraosseous lipoma (the more common variant) and true intraosseous hemangioma. It is not clear whether a hemangioma diagnosed by MRI must be further differentiated into true angioma or congenital angiectatic nevus.

MR Technique

Vertebral hemangioma can be identified on sagittal, coronal, and axial images. T1- and T2-weighted images with fat saturation should be obtained for lesion characterization and differentiation from lipoma.

MR Findings

Vertebral hemangiomas predominantly occur in the lower thoracic and upper lumbar regions and are seen